MJFAS MALAYSIAN JOURNAL OF FUNDAMENTAL AND APPLIED SCIENCES
PRINT ISSN: 2289-5981 | ONLINE ISSN: 2289-599X

RESEARCH ARTICLE

Copper oxide derived from copper(I) complex of 2-acetylpyridine-N(4)-(methoxy phenyl)thiosemicarbazone as an efficient catalyst in the reduction of 4-nitrophenol

Omar Abdullahi Wafudu Handy, Mohamad Shazwan Shah Jamil*, Mustaffa Shamsuddin

Department of Chemistry, Faculty of Science, Universiti Teknologi Malaysia, 81310 UTM Johor Bahru, Johor, Malaysia

** Corresponding author: shazwan.shah@utm.my*

Article history
Received 5 December 2019
Revised 10 Mac 2020
Accepted 9 April 2020
Published Online 15 June 2020

Graphical abstract

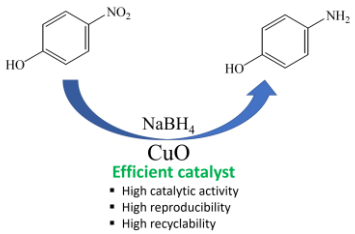

Abstract

A copper(I) complex of 2-acetylpyridine-N(4)-(methoxy phenyl)thiosemicarbazone was successfully synthesized and structurally characterized using Fourier transform infrared (FTIR), Ultraviolet-visible (UV-Vis) and nuclear magnetic resonance (NMR) spectroscopies, thermal gravimetric analysis (TGA) and CHN elemental analyses. The complex was converted into copper oxide in a simple, efficient, and cheap method *via* solid state thermal decomposition. Test of the catalytic performance of the copper(I) complex and copper oxide were in the reduction of 4-nitrophenol (4-NP) to 4-aminophenol (4-AP) shows that copper oxide has a higher catalytic activity (98.7%) compared to the copper(I) complex (78.2%). Optimization of the catalyst loading revealed that 1.0 mol% of catalyst was the most optimized amount with the highest conversion (98.7%) than any other amounts, 0.5 mol% (96.8%), 1.5 mol% (95.4%) and 2.0 mol% (89.6%). Recyclability and reproducibility tests of copper oxide prove that this catalyst was very efficient, exhibit excellent reproducibility with consistent catalytic performances and could be reused four times without significant decrease in the catalytic activities.

Keywords: Copper oxide, copper(I) complex, thiosemicarbazones, 4-nitrophenol reduction

INTRODUCTION

Copper oxide (CuO) is an important transition metal oxide with many practical applications such as catalysis, gas sensors, solar cells, battery materials and antimicrobial in biomedical studies [1, 2, 3, 4]. Due to its numerous applications, the synthesis of nanostructured CuO has also attracted considerable attention. Various synthetic methods have been reported for the preparation of CuO nanoparticles including electrochemical, hydrothermal, solvothermal, sonochemical, mechanochemical and biological methods [5, 6, 7, 8, 9]. Although these preparation methods are already established, however there are some disadvantages associated with these techniques. The electrochemical and chemical processes are quite expensive, involving some sophisticated equipment and require harsh conditions and the use of toxic chemicals. Biological approach on the other hand is cheaper, safer and environmental-friendly, however the process takes much longer time as the initial stage involves the extraction of biological resources [10]. Amongst all these techniques, the solid-state thermal decomposition of transition metal complexes as precursor is one of the simplest technique for preparing nanosized transition-metal oxides [11]. By selecting an appropriate precursor together with a rational calcinations procedure, products with nano sizes could be obtained. This method also has potential advantages, including high yield of pure products, absence of solvent, and exempting the need for special equipment.

In this paper, we describe the synthesis and characterisation of copper oxide from the thermal decomposition of copper(I) complex of 2-acetylpyridine-N(4)-(methoxy phenyl)thiosemicarbazone as novel precursor. The catalytic activity of the synthesized CuO was evaluated towards the reduction of 4-nitrophenol in the presence of sodium borohydride as a reducing agent.

EXPERIMENTAL

Materials and methods

All the chemicals and reagents used in this study were commercially purchased and used, as received without further purification. Solvents were distilled before use and dried over molecular sieves (4Å). All glassware were washed and dried overnight in an oven. The reactions were conducted under an inert atmosphere of nitrogen. The products obtained were collected using vacuum filtration and dried over silica gel in a desiccator before characterization. The synthesized products were characterized by melting point, UV-Vis, FTIR and ^{1}H NMR spectroscopies. The UV-Vis spectra were recorded in dimethylformamide (DMF)/chloroform ($CHCl_3$) solutions using a Shimadzu model UV-Vis probe 1800 spectrophotometer in the range of 200-800 nm. The infrared spectra were obtained using the FTIR Frontier-Elmer 1800 Model spectrophotometer in the range of 4000-400cm^{-1}. Solution state ^{1}H-NMR for the ligands and the complexes were recorded on a Bruker Avance 400 MHz spectrometer analyzer using deuterated chloroform ($CDCl_3$) and deuterated acetone d_6 as a solvent. Chemical shifts were verified, as δ values in part per million (ppm) relative to tetra-methyl silane (TMS) as the internal reference standard. Melting points were determined using Electro-thermal 1900 Model. The elemental analysis of carbon, hydrogen, nitrogen and sulphur, was elucidated according to the ligands and complexes

molecular weight. The thermographic analysis (TGA) was recorded on a Mettler Toledo TGA/SDTA851E instrument and X-Ray diffraction (XRD) patterns were recorded using a Bruker D8 Advance powder diffractometer with a Cu Kα radiation (λ = 1.54060 Å) operating at 40 kV and 30 mA in the 2θ range from 10º to 90º.

Preparation of thiosemicarbazide

N(4)-(methoxyphenyl)thiosemicarbazide was prepared by mixing N(4)-(Methoxy-phenyl)isothiocyanate (3 mL, 3.54 g, 21.46 mmol) with hydrazine monohydrate (5 mL, 5.15 g, 100 mmol). The reaction mixture was stirred at room temperature for 2 hours. A white precipitate formed was collected via vacuum filtration, washed with cold diethyl ether, and dried in a desiccator over silica gel. The silky white product was recrystallized from methanol. Yield 83.9%. Melting point: 152-153ºC. This value is consistent with the previous reported data [12].

Synthesis of thiosemicarbazone ligand

N(4)-(methoxyphenyl)-thiosemicarbazide (0.3624 g, 2 mmol) in ethanol (15 mL) was mixed with 2-acetylpyridine (0.24 mL, 0.242 g, 2 mmol) in a round bottom flask. Acetic acid (0.2 mL) was added to the mixture and refluxed in nitrogen flow for 4 hours. A yellowish-orange product formed was filtered and washed with ethanol. Then, the product was washed with diethyl ether and dried over silica gel in a desiccator. Yield, 0.2401 g, 87.0%. Colour: Yellowish-orange. Melting point: 173-174ºC. This value is consistent with the previous reported data [12].

Preparation of tris-(triphenylphosphine)copper(I) nitrate

In a 25 mL beaker, copper(I) nitrate trihydrate (0.365 g, 1.5 mmol) was dissolved in ethanol (10 mL). In another beaker, triphenylphosphine (1.965 g; 7.5 mmol) was also dissolved in ethanol (30 mL) and warmed. The two solutions were mixed in a 100 mL round bottom flask and refluxed for 1 hour**.** The resulting mixture was allowed to cool to room temperature. The white product was filtered, washed with cold ethanol and followed by diethyl ether, then dried in a desiccator over silica gel. Yield 0.7796 g, 85.4%. Melting point: 154-156°C. This value is in good agreement with the published data [13].

Synthesis of 2-acetylpyridine-N(4)-(methoxyphenyl) thiosemicarbazone-tris-(triphenyl-phosphine)copper(I) nitrate

Tris-(triphenylphosphine)copper(I) nitrate (0.912g, 1 mmol) was dissolved in dichloromethane (10 mL) and stirred for 30 minutes under nitrogen flow at room temperature. To the solution, a solution of 2-acetylpyridine-N(4)-(methyl phenyl)thiosemicarbazone (0.181g, 1mmol) dissolved in dichloromethane (10 mL) was added. The resulting mixture turned to reddish colour and was stirred at room temperature for 3 hours. Then, the solution reduced to a small volume under vacuum. Brown coloured complex was developed by diffusion of diethyl ether into the filtrate. Yield: 78% Colour: Brown crystals, melting point 259 – 260ºC. Anal Calcd for $CuC_{69}H_{61}N_5P_3O_3S$ (1192.807 g/mol: Calcd: C, 69.01, H, 5.20, N, 5.21, S, 2.67 %) Found: C, 69.14, H, 5.15, N, 5.87, S, 2.69 %.

Thermal decomposition of 2-acetylpyridine-N(4)-thiosemicarbazone of copper(I) nitrate to copper oxide

0.5 g of the complex was measured and calcined in hot air furnace Carbolite model at variable temperatures of 500, 600, 700 and 800ºC between 30ºC to 900ºC at 10^0C min^{-1} for 3h. These temperatures were chosen because the ligands decompose at temperature above 500°C. The product was best calcined between 700 – 800ºC and purified by washing with 2 M ammonium hydroxide solution to remove phosphate $(PO_4)^{-2}$ and dried for 2 hours in an oven at 100ºC. The copper oxide was confirmed by XRD powder diffraction method using Rigaku diffractometer Smart lab model, X-ray diffractometer with Cu Kα radiation 2θ ranging from 10º to 90º at room temperature heating rates of 10°C min^{-1} for 2 hours at wavelength of 1.54 Å.

Catalytic performance of the catalyst in the reduction of 4-nitrophenol

A freshly prepared aqueous $NaBH_4$ (1 mL, 0.2 mol) was mixed with an aqueous solution of 4-NP (3 mL, 0.01 mol) in a quartz cuvette with 1.0 cm path length and 4 mL volume. The solution was prepared using deionized water. The colour of the solution changed immediately to deep-yellow colour upon addition of $NaBH_4$. Then the catalyst (1 mol%) was added to the mixture, and the initial yellow colour of the solution turned to colourless as the reaction proceeded. The progress of the reduction was evaluated by UV-Vis spectrophotometer in the scanning range between 200 nm to 500 nm. The absorbance for the 4-nitrophenolate ion peak at λ = 400 nm was recorded in every cycling over 2 min at room temperature. A standard calibration curve was plotted based on six concentrations of 4-NP solutions with $NaBH_4$ ranging from 0.01 – 0.1 mM. The percentage of conversion from 4-NP to 4-AP was determined by calculation from the absorbance data using the following equation:

$$\text{Percentage conversion} = \frac{\text{Initial Abs - Final Abs}}{\text{Initial Abs}} \times 100\%$$

Isolation of the product

The progress of the conversion reaction was monitored by UV-Vis spectroscopy. When the conversion was completed, the product was isolated by the following procedure. Firstly, the product was diluted with diethyl ether (30 mL) and separated using liquid-liquid extraction. The extraction steps were repeated three times, and the diethyl ether fractions containing the product (4-AP) were combined and dried using anhydrous sodium sulphate (Na_2SO_4). Then, diethyl ether was evaporated using a rotary evaporator. Purification of 4-aminophenol by a silica gel column chromatography was done by eluding the product with solvent composed of hexane and ethyl acetate in a ratio of 1:2. Each eluent was loaded on a thin layer chromatography (TLC) plate together with the 30 mL 4-AP standard. The fraction containing 4-AP were combined, and solvents were evaporated using a rotary evaporator. The product was characterized by NMR and UV-Vis spectroscopy.

Recovery of the catalyst

The catalyst was recovered by centrifuging the mixture at 4000 rpm for 40 min. After this time, the catalyst was settled at the bottom of the centrifugation tube and recovered by decanting the solution. The recovered catalyst was washed with deionized water twice and dried over silica gel for subsequent experiments.

Optimization of the amount of copper oxide in the reduction of 4-nitrophenol

The cataytic experiments were repeated three times under the same condition as the model reactions, except that the catalyst amount was varied (0.5 mg, 1.0 mg, 1.5 mg and 2.0 mg). Percentage conversion for each catalyst amount was determined from the UV-Vis spectroscopic data.

Recyclability test of copper oxide in the reduction of 4-nitrophenol

Recycle experiments were performed to test the reusability of the copper oxide catalyst. The recyclability test was performed by carrying out the reaction under the same conditions as the model reaction. After the first run, the catalyst was separated from the reaction mixture by centrifugation. The catalyst was washed twice with deionized water to remove any residue from the catalytic reaction mixture. The separated catalyst was dried in a vacuum desiccator and reused again. In the subsequent run, the same amount of 4-NP and a freshly prepared $NaBH_4$ were used. The percentage conversion of the 4-NP was calculated and compared with the first run.

Reproducibility test of copper oxide in the reduction of 4-nitrophenol

The catalytic experiments were repeated three times by performing the reaction under the same conditions as the model reaction. For each

reaction, a fresh catalyst was used to determine the reproducibility of copper oxide.

RESULTS AND DISCUSSION

Synthesis of 2-acetylpyridine-N(4)-thiosemicarbazone ligand and its copper(I) complex

The first stage involves the preparation of thiosemicarbazone ligand, from thiosemicarbazide. Thiosemicarbazide was prepared by reacting N(4)-(methoxy-phenyl)isothiocyanate with hydrazine monohydrate at room temperature for 2 hours. The preparation scheme is shown in Fig. 1. The resulting product, N(4)-(methoxyphenyl)-thiosemicarbazide was then reacted with 2-acetylpyridine in ethanol for 4 hours, as decipted in Fig.2 This ligand was characterized using UV-Vis, IR and NMR spectroscopies and characterization data were in good agreement with the literature values [12].

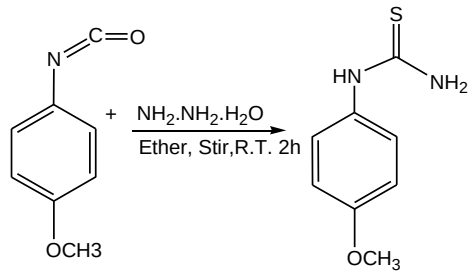

Fig. 1 Scheme for the preparation of N(4)-methoxyphenyl)-thiosemicarbazide

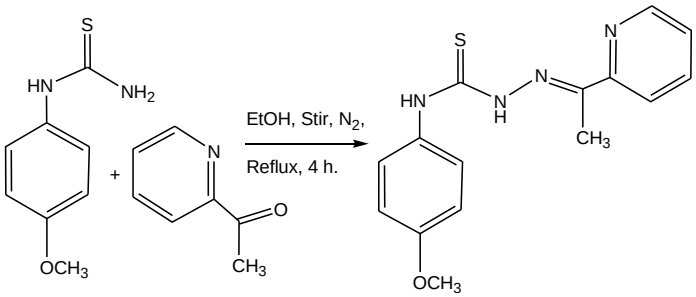

Fig. 2 Scheme for the preparation of 2-acetylpyridine-N(4)-(methoxyphenyl)thiosemicarbazone

Having synthesized the ligand, the next stage involves the synthesis of the copper(I) complex. The copper source for this reaction is tris-(triphenylphosphine)copper(I) nitrate, which can be prepared from triphenylphosphine and copper(I) nitrate trihydrate, as shown in Fig. 3. The characterization data of this complex are consistent with the previous reported data [13].

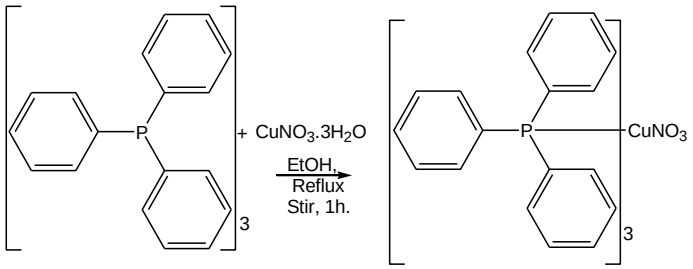

Fig. 3 The preparation scheme of tris-(triphenylphosphine) copper(I) nitrate

The schematic diagram for the preparation of copper(I) complex is displayed in Fig. 4. The copper source, tris-(triphenylphosphine) copper(I) nitrate was reacted with the ligand, 2-acetylpyridine-N(4)-(methylphenyl)thiosemicarbazone in dichloromethane and stirred at room temperature for 3 hours. The solvent was removed under vacuum and the product was collected as brown crystals with yield of 78%.

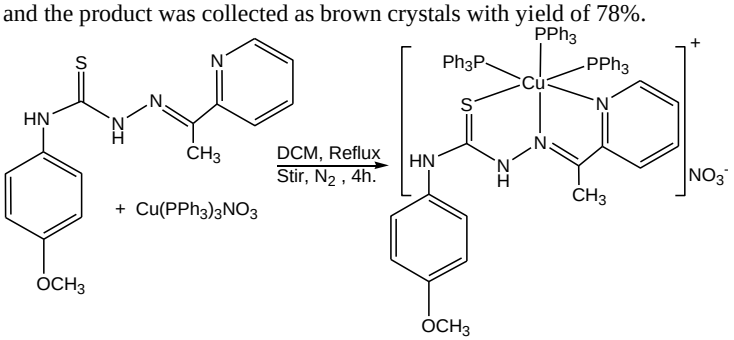

Fig. 4. The schematic diagram for preparation of 2-acetylpyridine N(4)-(methoxyphenyl)thiosemicarbazone copper(I) nitrate

Characterization of thiosemicarbazone ligand and its complex

Thiosemicarbazone and its copper(I) complex were successfully synthesized and characterized by several characterization techniques, elemental analysis (CHN), UV-Visible, Fourier-transform infrared (FT-IR), nuclear magnetic resonance spectroscopic (^{1}H-NMR) techniques. Both the ligand and its complex are yellow and brown in colour respectively, which are similar to the characteristic of other common compounds of thiosemicarbazone [14]. The CHN elemental analyses data of both ligand and complex are consistent with the calculated data, as shown in Table 1.

Table 1. Elemental analysis of CHN of ligand and its complex

Elemental	C. Found/Calcd	H. Found/Calcd	N. Found/Calcd
Ligand	60.23/60.00	5.41/5.37	18.69/18.66
Complex	69.06/69.01	5.03/5.07	5.92/5.96

The electronic absorption spectra of both ligand and its complex were recorded in a solution of chloroform (10^{-3} M) in the wavelength range of 200 – 800 nm. In the spectra of the free ligand, the band at 255 nm was assigned to n – π* transitions of thioamide, whilst the absorption at 317 nm corresponds to a π – π* transition of the pyridine ring and azomethine [13, 15]. The absoprtion bands of the complex appear at 265 nm owing to n – π*, and the other one at 428 nm corresponds to π – π* transitions. By comparing the frequency of free ligands and the corresponding copper(I) complexes, the electronic transitions of n – π* are shifted to a higher value due to the formation of the complexes and coordination of the ligand to the copper. This data is consisent with other similar copper complexes [16, 17, 18]. Figure 5 displays the UV-Vis spectra of the ligand and its complex, marked as black and red respectively.

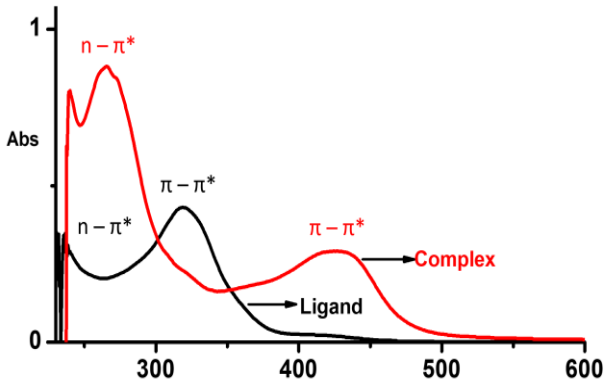

Fig. 5 The UV-Vis spectra of thiosemicarbazone ligand (black) and the copper(I) complex of thiosemicarbazone (red).

In addition, Figure 6 shows the IR spectra of the ligand and the complex, while the IR frequencies of selected groups in both the ligand and complex are given in Table 2. The bands observed in the free ligand, at 1610 and 1526 cm^{-1}, correspond to ν(C=N) of pyridine (py) and azomethine (azo). These bands are shifted to 1584 and 1509 cm^{-1} in the complex, indicating coordination of azomethine and nitrogen to the copper, which is consistent with the other literature data [19, 20]. Due to the displacement of electron density from N to Cu atom, this leads to the weakening of the ν(C=N), as seen in other works [21, 22]. The band observed at 833cm^{-1} in the free ligand which attributed to ν(C=S) was not seen in the spectrum of the complex. A new group appeared at lower energy (743 cm^{-1}) indicating coordination of sulphur atom to copper [23]. The appearance of bands at 1446 cm^{-1} and 694 cm^{-1} also signify the presence of triphenylphosphine (PPh_3) in the complex. The absorption band at 1384 cm^{-1} in the complex indicates the presence of free nitrate, NO_3, which in agreement with other published works [24, 25, 26].

Table 2 Selected IR data of the ligand and copper(I) complex

Compd/Freq.	Pyridine (py) ν(C=N) /cm^{-1}	Azomethine (azo) ν(C=N) /cm^{-1}	Thio ν(C=S) /cm^{-1}
Ligand	1610	1526	833
Complex	1584	1509	743

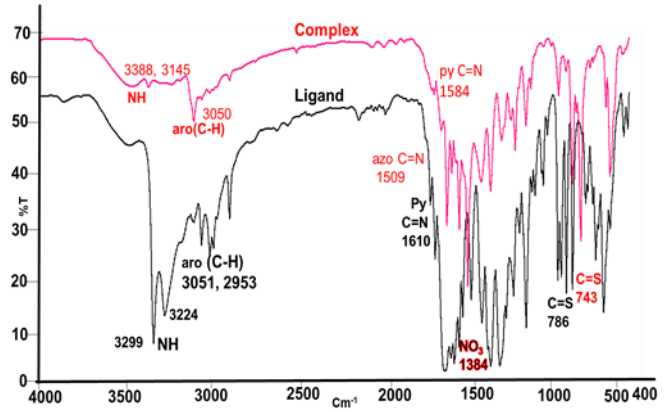

Fig. 6 The IR spectra of thiosemicarbazone ligand (black) and the copper(I) complex of thiosemicarbazone (red).

Meanwhile, Figures 7 and 8 portray the ^{1}H-NMR spectra of the ligand and complex respectively, while some selected spectroscopic data are given in Table 3. The resonance of phenyl protons in the free ligand shifted from δ_H 9.6 to 9.2 ppm in the complex, whilst the peak of the imine protons in the ligands moved from δ_H 9.9 to 12.0 ppm, indicating the coordination of the ligand to the copper. The downfield shift of the imine protons of the complex compared to the free ligand is attributed to deshielding effect, as the electron density around the imine proton decreases upon coordination of the ligand to copper ion [20, 27]. In addition, two sharp singlets appeared at δ_H 3.8 ppm, and 2.5 ppm are assigned to methoxy (C-OCH_3) and methyl (CH_3) equivalent protons respectively, in both ligand and complex.

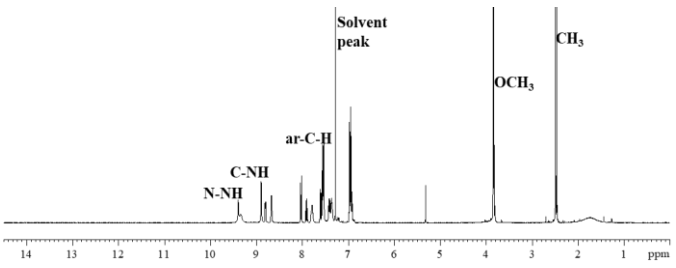

Fig. 7 The ^{1}H NMR spectrum of the ligand.

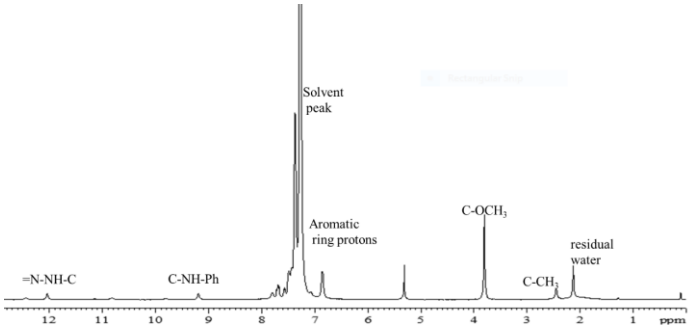

Fig. 8 The ^{1}H NMR spectrum of copper(I) complex.

Table 3 ^{1}H-NMR of ligand and its complex.

Compd	δ(N-NH-C) /ppm	δ(NH-Ar) /ppm	δ(Ar-H) /ppm	δ(OCH_3) /ppm	δ(CH_3) /ppm
Ligand	9.9	9.6	6.8-8.8	3.8	2.5
Complex	12.0	9.2	6.8-7.8	3.8	2.5

Thermal gravimetric analysis

Prior to the calcination of the complex, thermal gravimetric analysis was conducted to determine the decomposition temperature. 2.0 g of the complex was measured for the thermographic analysis using 4000 Perkin Elmer model thermographic analyser instrument under a nitrogen atmosphere with a heating rate of 10°C min^{-1} over the temperature range from 100 to 900°C. Thermal gravimetric analysis (TGA) measures weight/mass change (loss or gain) and the rate of weight change as a function of temperature, time and atmosphere. Measurement is used primarily to determine the thermal composition of materials and to predict their thermal stability**.** The thermal properties of the ligand and its metal complex were investigated using this method. Figure 9 shows the recorded TGA and differential gravimetric analysis (DTA) curves of ligand (a) and copper(I) complex (b). Copper(I) complex was heated under a nitrogen atmosphere with a heating temperature range of 30 - 950°C, at rate of 10°C/min. The thermal decomposition of the ligand and its metal complex showed three stages and these were irreversible. The first stage of the TGA degradation was from 70 – 170°C, which corresponded to the lost of lattice water with the mass loss of 15.0%, while the second stage occured in the temperature range between 200 – 300°C, indicating the removal of triphenylphosphine with mass lost of 65.0% associated with exothermic peaks at 180°C and 310°C. The final decomposition stage occurred between the temperature range of 340 - 620°C, which attributed to the free ligand with weight loss of 15.0%, leaving stable copper oxide as a residue between 640 - 950°C, consistent with the previous data [28, 29]. Ning and co-workers studied the thermal stability of a copper dicarboxylate ligand and they observed that the decomposition occurred in three stages. The first stage involved the loss of water from 130 - 185°C (Calc. 18.76%). The second weight loss happened in the range of 188 to 600°C, which was due to the decomposition of an organic ligand (Calc., 59.1%). The final thermal product after 450 °C was CuO particles (Calc., 27.6%) [30]. Based on this observation, solid state thermal decomposition method provides a simple, efficient and inexpensive way of producing copper oxide.

X-ray diffraction (XRD) of the copper oxide

Copper oxide obtained from the thermal decomposition of copper(I) complex was confirmed by the characteristic peaks observed in the XRD pattern, as shown in Fig. 10. XRD analysis showed intense peaks at 35.45°, 35.55°, 38.74°, 38.93°, 48.74°, 51.38°, 58.30°, 61.56° and 65.84°, which correspond to (-011), (002), (110), (202), (-202), (202), (202), (113), (-022) and (113) respectively. The observed diffraction reflections were comparable with other literature data [31, 32]. All diffraction peaks could be indexed as the typical monoclinic structure and no extra diffraction peaks of other phases were observed [28, 30].

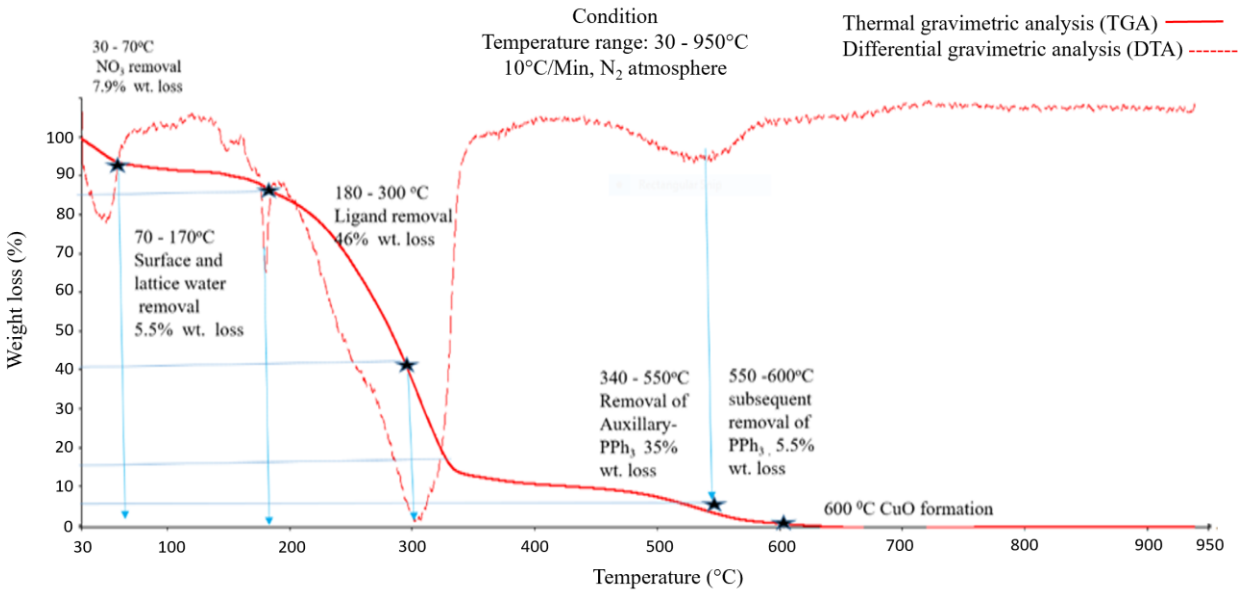

Fig. 9 The TGA analysis of copper(I) complex.

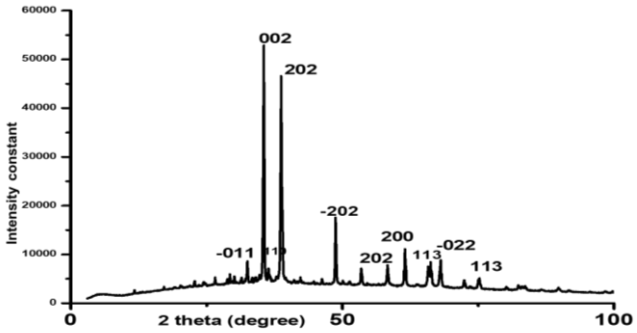

Fig. 10 The XRD pattern of copper oxide.

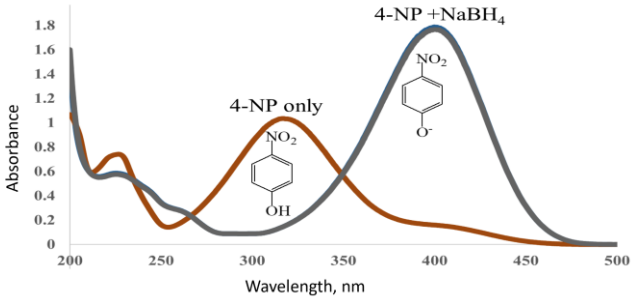

Fig. 12 Monitoring the progress of reaction using UV-Vis spectroscopy.

Catalytic activity of copper-based catalysts in the reduction of 4-nitrophenol

Reduction of 4-nitrophenol (4-NP) to 4-aminophenol (4-AP) was selected as a model reaction to evaluate the catalytic activity of copper-based catalysts. This reaction provides a straightforward assessment of catalysts using the kinetic parameters extracted from the real-time spectroscopic monitoring of an aqueous solution by using UV-Visible spectrophotometer. In this study, the catalytic activity of copper(I) complex and its oxide were evaluated in the reduction of 4-NP at room temperature, in the presence of $NaBH_4$, as presented in Fig. 11 below. When 4-NP was mixed with $NaBH_4$, the solution became yellowish and has a maximum absorbance at 400 nm due to the formation of 4-nitrophenolate anion. This peaks is very distinctive in the UV-Vis spectrum as shown in Fig. 12. Upon the addition of the catalyst, the peak at 400 nm was started to decrease whilst a new peak around 300 nm was appeared at the same time. The new peak at 260 nm was due to an absorbance of the reaction product, 4-AP. Time was recorded for the complete disappearance of the peak at 400 nm. The time taken for the disappearance of the peak at 400 nm is proportional to the catalytic performance of the catalyst used.

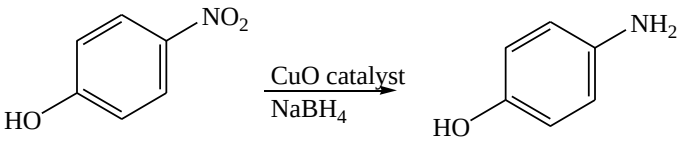

Fig. 11 The schematic diagram for the reduction of 4-nitrophenol to 4-aminophenol, catalyzed by copper-based catalyst.

Fig. 13 shows the reduction of 4-NP by copper(I) complex. Based on this graph, the conversion was measured as 78.2% over 420 min. The experiment was repeated by using copper oxide as catalyst and the conversion was determined as 98.7% at 16 minutes (see Fig. 14). Based on these values, it shows that catalytic activity of copper oxide-derived from copper(I) complex was higher than those of the complex.

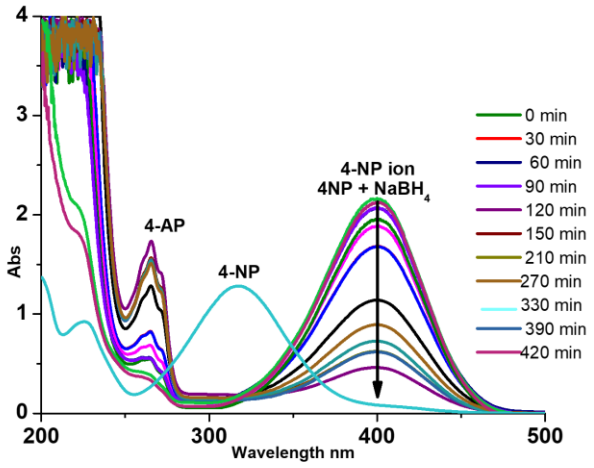

Fig. 13 The UV-Vis spectrum of the reduction of 4-NP with copper(I) complex.

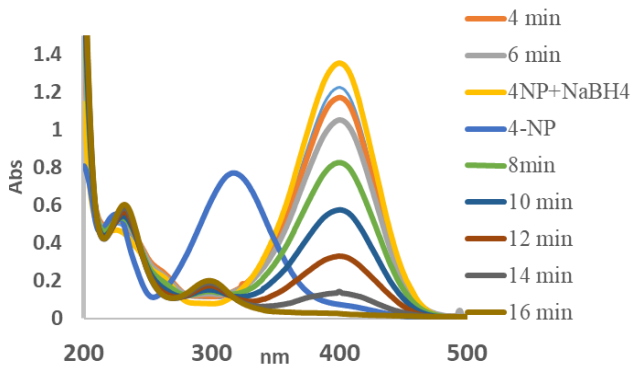

Fig. 14 UV-Vis spectrum of the reduction of 4-NP catalysed by copper oxide.

For quantitative analysis, a calibration curve was constructed with 4-NP solution. A linear regression equation of y=24.357x + 0.025 with correlation coefficient of 0.997 in the concentration range of 0.01–0.12 mM was obtained, as shown in Fig. 15. Based on this equation, the conversion yield of 4-NP to 4-AP was measured to be 98.7%. A reaction rate was measured from the plot between ln (A_t/A_0) versus time (sec). Herein, the 4-NP concentrations at time t=0 and time, t were expressed as A_0 and A_t, respectively. It was shown that there was a linear relationship between ln (At/A0) and time (sec), suggesting that the reaction followed a pseudo-first order kinetics with a rate constant value of 1.7 x 10^{-3} s^{-1} (see Fig. 16).

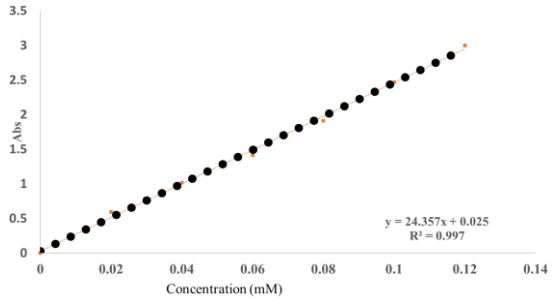

Fig. 15 Calibration curve of 4-NP at different concentrations.

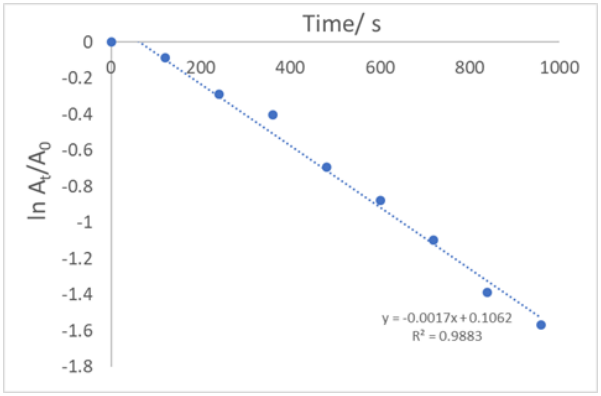

Fig. 16 A graph showing ln (A_t/A_0) versus time (s).

Optimization, recyclability and reproducibility of copper oxide

Due to the efficiency of copper oxide as a catalyst in the reduction of 4-NP to 4-AP, further investigations were carried out to determine the catalytic properties of copper oxide. In this work, optimization of the catalyst amount of copper oxide was done by varying the amount of catalyst loading in the reduction experiment. For this purpose, different amounts of copper oxide were used in each experiments whilst the other reaction conditions were kept constant. The conversions were measured for each amount and these data are tabulated in Table 4 below. According to the results, the catalytic loading of 1.0 mol% was the optimized amount due to its highest conversion, as compared to other catalytic amounts.

Table 4 The optimization copper oxide with different catalyst amount.

Catalyst amount / mol%	Conversion / %
0.5	96.8
1.0	98.7
1.5	95.4
2.0	89.6

The recyclability of the copper oxide for reduction of 4-NP was investigated by employing the used copper oxide as a catalyst in the successive cycles of reaction. The used copper oxide was collected by centrifugation and washed thoroughly with deionized water to remove any residues from previous catalytic reactions, so that it can be reuse again in the next repetitive runs. These recyclability tests were repeated three times, and the results are illustrated in Table 5. Based on the results, copper oxide showed a relatively good catalytic activity even in the forth cycle, with 91.6% conversion. The slight decrease in the catalytic performance may be due to the loss of catalyst mass during the catalyst recovery process. Nevertheless, this proves tht copper oxide is an efficient catalyst in the reduction of 4-NP and could be reused three times without significant decrease in the catalytic activities.

Table 5 Recyclability test of copper oxide.

	Conversion / %
First cycle	98.7
Second cycle	96.9
Third cycle	94.9
Forth cycle	91.6

In addition, the reproducibility test was also performed to evaluate the consistency and accuracy of the conversions. This is done by repeating the reduction of 4-NP under the same conditions with fresh samples of copper oxide in each run. The conversions for each run were measured and tabulated in Table 6. The results indicate that copper oxide shows a high reproducibilty data with consistent catalytic ativity.

Table 6 Reproducibility test of copper oxide

	Conversion / %
First, run	98.7
Second run	98.4
Third run	98.8
Forth run	98.6

Purification and characterization of product

To determine the successful conversion of 4-NP to 4-AP, the product, 4-AP must be purified and characterized. The product was purified by a silica gel column chromatography and characterized by ^{1}H NMR spectroscopy techniques. Fig. 20 shows the proton NMR spectrum of the product, 4-aminophenol. The appearance of signals at δ_H 6.49 and 4.39 ppm are due to the aromatic proton and amino protons respectively. Meanwhile, the extra two peaks at 3.5 and 2.5 ppm correspond to the solvent and residual water respectively. The proton NMR of the starting material, 4-nitrophenol is shown in Fig. 21 for comparison. The full NMR assignment is illustrated as following and these data are consistent with the standard 4-AP [33].

4-Aminophenol (purified): 1H NMR (400 MHz, DMSO): δH = 8.36 (s, 1H), 6.47 (d, *J* = 8.4 Hz, 2H), 6.42 (d, *J* = 8.4 Hz, 2H), 4.35 (s, 2H).
4-Aminophenol (standard): 1H NMR (400 MHz, DMSO): δH = 8.37 (s, 1H), 6.50 (d, *J* = 8.4 Hz, 2H), 6.44 (d, *J* = 8.4 Hz, 2H), 4.39 (s, 2H).

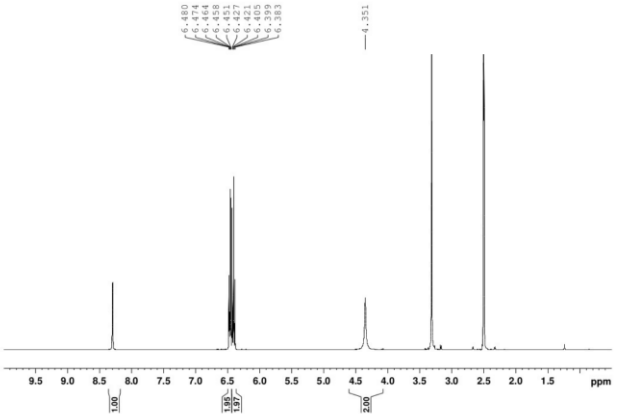

Fig 17 [1]H-NMR spectrum of the purified 4-aminophenol.

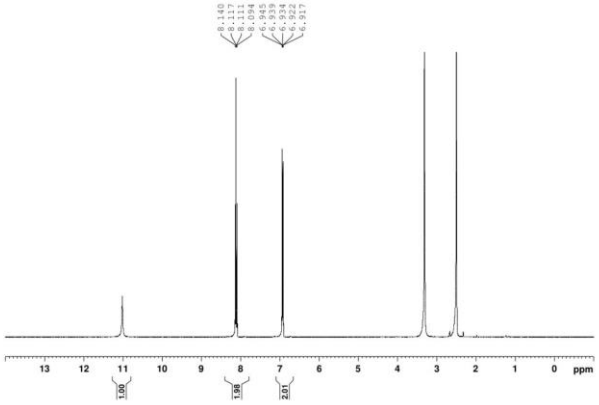

Fig 18 [1]H-NMR spectrum of 4-nitrophenol.

CONCLUSION

A new copper(I) complex of 2-acetylpyridine-N(4)-(methyl phenyl)thiosemicarbazone-tris-(triphenylphosphine) nitrate was successfully synthesized and charazterized by various spectroscopic techniques such as Fourier transform infrared, (FT-IR), UV-visible, (UV), proton nuclear magnetic resonance ([1]H-NMR). Thermal graphic analysis (TGA) and molar conductivity were performed to investigate the properties of the complex. Solid state thermal decomposition technique was successfully employed to convert the complex into copper oxide. This method was simple, efficient, solventless, low cost and environmentally friendly without using any toxic chemicals. The results showed that copper oxide has a higher catalytic activity than the complex, with 97.1 and 78.7% conversions respectively. Optimization of copper oxide catalyst was performed by varying the catalyst amount, 0.5, 1.0, 1.5 and 2.0 mol% and the conversions were measured as 96.7, 98.7, 95.4 and 89.6% respectively. The result indicates that 1.0 mg of catalyst was the optimized catalyst loading for the reduction of 4-nitrophenol to 4-aminophenol. Recyclability and reproducibility tests were performed and the results proved that copper oxide was easily recovered, maintained high and consistent catalytic activities over four cycles without any significant decrease in the conversion of the product.

ACKNOWLEDGEMENT

The authors would like to thank the Universiti Teknologi Malaysia for the research facilities. O. A. W. H. acknowledge the Federal Government of Nigeria for providing Tetfund assistant through the Federal Polytechnic, Mubi- Adamawa State, to pursue his PhD studies.

REFERENCES

[1] Li, W., Cui, X., Junge, K., Surkus, A. E., Kreyenschulte, C., Bartling, S., Beller, M. (2019). General and chemoselective copper oxide catalysts for hydrogenation reactions. *ACS Catalysis*, *9*(5), 4302-4307.

[2] Liu, X., Cui, S., Qian, M., Sun, Z., Du, P. (2016). In situ generated highly active copper oxide catalysts for the oxygen evolution reaction at low overpotential in alkaline solutions. *Chemical communications*, *52*(32), 5546-5549.

[3] Bhaumik, A., Haque, A., Karnati, P., Taufique, M. F. N., Patel, R., Ghosh, K. (2014). Copper oxide based nanostructures for improved solar cell efficiency. *Thin Solid Films*, *572*, 126-133.

[4] Grigore, M. E., Biscu, E. R., Holban, A. M., Gestal, M. C., Grumezescu, A. M. (2016). Methods of synthesis, properties and biomedical applications of CuO nanoparticles. *Pharmaceuticals*, *9*(4), 75.

[5] Velusamy, V., Palanisamy, S., Kokulnathan, T., Chen, S. W., Yang, T. C., Banks, C. E., Pramanik, S. K. (2018). Novel electrochemical synthesis of copper oxide nanoparticles decorated graphene-β-cyclodextrin composite for trace-level detection of antibiotic drug metronidazole. *Journal of Colloid and Interface Science*, *530*, 37-45.

[6] Kumar, K. Y., Muralidhara, H. B., Nayaka, Y. A., Hanumanthappa, H., Veena, M. S., Kumar, S. K. (2014). Hydrothermal synthesis of hierarchical copper oxide nanoparticles and its potential application as adsorbent for Pb (II) with high removal capacity. *Separation Science and Technology*, *49*(15), 2389-2399.

[7] Saravanan, S., Sivasankar, T. (2016). Effect of ultrasound power and calcination temperature on the sonochemical synthesis of copper oxide nanoparticles for textile dyes treatment. *Environmental Progress & Sustainable Energy*, *35*(3), 669-679.

[8] Ameri, B., Davarani, S. S. H., Roshani, R., Moazami, H. R., Tadjarodi, A. (2017). A flexible mechanochemical route for the synthesis of copper oxide nanorods/nanoparticles/nanowires for supercapacitor applications: The effect of morphology on the charge storage ability. *Journal of Alloys and Compounds*, *695*, 114-123.

[9] Sharma, J. K., Akhtar, M. S., Ameen, S., Srivastava, P., Singh, G. (2015). Green synthesis of CuO nanoparticles with leaf extract of Calotropis gigantea and its dye-sensitized solar cells applications. *Journal of Alloys and Compounds*, *632*, 321-325.

[10] Verma, N., Kumar, N. (2019). Synthesis and biomedical applications of copper oxide nanoparticles: an expanding horizon. *ACS Biomaterials Science & Engineering*, *5*(3), 1170-1188.

[11] Monadi, N., Saeednia, S., Iranmanesh, P., Ardakani, M. H., Sinaei, S. (2019). Preparation and characterization of copper oxide nanoparticles through solid state thermal decomposition of an aqua nitrato copper (II) complex with a tridentate schiff-base ligand as a new precursor. *Nanoscience & Nanotechnology-Asia*, *9*(1), 92-100.

[12] Manikandan, R., Viswanathamurthi, P., Velmurugan, K., Nandhakumar, R., Hashimoto, T., Endo, A. (2014). Synthesis, characterization and crystal structure of cobalt (III) complexes containing 2-acetylpyridine thiosemicarbazones: DNA/protein interaction, radical scavenging and cytotoxic activities. *Journal of Photochemistry and Photobiology B: Biology*, *130*, 205-216.

[13] Ramachandran, R., Prakash, G., Vijayan, P., Viswanathamurthi, P., & Malecki, J. G. (2017). Synthesis of heteroleptic copper (I) complexes with phosphine-functionalized thiosemicarbazones: An efficient catalyst for regioselective N-alkylation reactions. *Inorganica Chimica Acta*, *464*, 88-93.

[14] Omar, S. A., Ravoof, T. B., Tahir, M. I. M., Crouse, K. A. (2014). Synthesis and characterization of mixed-ligand copper (II) saccharinate complexes containing tridentate NNS Schiff bases. X-ray crystallographic analysis of the free ligands and one

complex. *Transition Metal Chemistry*, *39*(1), 119-126.

[15] Ibrahim, D., Ndahi, N. P., Paul, B. B., Handy, O. W. Synthesis, characterization and antimicrobial activity of 2-Aminopyridine-cephalexin schiff base and its Mn (II), Co (II) AND Cu (II) complexes.

[16] Ibrahim, A. B., Farh, M. K., Mayer, P. (2018). Copper complexes of new thiosemicarbazone ligands: Synthesis, structural studies and antimicrobial activity. *Inorganic Chemistry Communications*, *94*, 127-132.

[17] Rogolino, D., Cavazzoni, A., Gatti, A., Tegoni, M., Pelosi, G., Verdolino, V., ...Carcelli, M. (2017). Anti-proliferative effects of copper (II) complexes with hydroxyquinoline-thiosemicarbazone ligands. *European journal of medicinal chemistry*, *128*, 140-153.

[18] Kallus, S., Uhlik, L., van Schoonhoven, S., Pelivan, K., Berger, W., Enyedy, É. A., ... Keppler, B. K. (2019). Synthesis and biological evaluation of biotin-conjugated anticancer thiosemicarbazones and their iron (III) and copper (II) complexes. *Journal of inorganic biochemistry*, *190*, 85-97.

[19] Hakimi, M., Moeini, K., Mardani, Z., & Takjoo, R. (2014). Synthesis and Spectral Study of a Copper (I) Complex,[Cu (L)(PPh3) 2], with NS-Donor Ligand. *Phosphorus, Sulfur, and Silicon and the Related Elements*, *189*(5), 596-605.

[20] Jadhav, A. N. & Chavan, S. S. (2014). Alkynyl functionalized iminopyridine copper(I) phosphine complexes: Synthesis, spectroscopic characterization and photophysical properties. *Journal of Luminescence*, 148, 296–302.

[21] Chavan, S. S., Sawant, S. K., Pawal, S. B., More, M. S. (2016). Copper (I) complexes of 2-methoxy-(5-trifluoromethyl-phenyl)-pyridine-2yl-methylene-amine: Impact of phosphine ancillary ligands on luminescence and catalytic properties of the copper (I) complexes. *Polyhedron*, *105*, 192-199.

[22] Favarin, L. R., Rosa, P. P., Pizzuti, L., Machulek Jr, A., Caires, A. R., Bezerra, L. S., ... & dos Anjos, A. (2017). Synthesis and structural characterization of new heteroleptic copper (I) complexes based on mixed phosphine/thiocarbamoyl-pyrazoline ligands. *Polyhedron*, *121*, 185-190.

[23] Liu, T., Sun, J., Tai, Y., Qian, H., & Li, M. (2017). Synthesis, spectroscopic characterization, crystal structure, and biological evaluation of a diorganotin(IV) complex with 2-acetylpyridine N4-cyclohexylthiosemicarbazone. *Inorganic and Nano-Metal Chemistry*, 47(6), 813–817.

[24] Chen, J. L., Zeng, X. H., Luo, Y. S., Wang, W. M., He, L. H., Liu, S. J., ... & Wong, W. Y. (2017). Synthesis, structure, and photophysics of copper (i) triphenylphosphine complexes with functionalized 3-(2′-pyrimidinyl)-1, 2, 4-triazole ligands. *Dalton Transactions*, *46*(38), 13077-13087.

[25] Lobana, T. S., Kaushal, M., Virk, R. K., Garcia-Santos, I., & Jasinski, J. P. (2018). Thiosemicarbazonates of copper: Crystal structures of [(furan-2-acetaldehyde-N-phenyl-thiosemicarbazonato)][bis (triphenylphosphine)] copper (I) and [bis (furan-2-formaldehyde-N-phenyl-thiosemicarbazonato)] copper (II). *Polyhedron*, *152*, 49-54.

[26] Gunasekaran, N., Bhuvanesh, N. S. P., & Karvembu, R. (2017). Synthesis, characterization and catalytic oxidation property of copper (I) complexes containing monodentate acylthiourea ligands and triphenylphosphine. *Polyhedron*, *122*, 39-45.

[27] Jamil, M. S. S., Alkaabi, S., & Brisdon, A. K. (2019). Simple NMR predictors of catalytic hydrogenation activity for [Rh (cod) Cl (NHC)] complexes featuring fluorinated NHC ligands. *Dalton Transactions*, *48*(25), 9317-9327.

[28] Li, S. X., Luo, P., & Jiang, Y. M. (2017). Copper complexes with 4 (3H)-quinazolinone: Thermal gravimetric analysis and anticancer activity of [Cu (L) 2 (H 2 O) 2 (NO 3) 2],[Cu (L–)(NO 3)] n, and [Cu (L) 2 (H 2 O) 2 (Cl) 2]. *Russian Journal of Coordination Chemistry*, *43*(4), 238-243.

[29] Rajalakshmi, S., Vimalraj, S., Saravanan, S., Preeth, D. R., Shairam, M., & Anuradha, D. (2018). Synthesis and characterization of silibinin/phenanthroline/neocuproine copper (II) complexes for augmenting bone tissue regeneration: an in vitro analysis. *JBIC Journal of Biological Inorganic Chemistry*, *23*(5), 753-762.

[30] Rauf, A., Ye, J., Zhang, S., Shi, L., Akram, M. A., & Ning, G. (2019). Synthesis, structure and antibacterial activity of a copper (II) coordination polymer based on thiophene-2, 5-dicarboxylate ligand. *Polyhedron*, *166*, 130-136.

[31] Nordin, N. R., & Shamsuddin, M. (2019). Biosynthesis of copper (II) oxide nanoparticles using Murayya koeniggi aqueous leaf extract and its catalytic activity in 4-nitrophenol reduction. *Malaysian Journal of Fundamental and Applied Sciences*, *15*, 218-224.

[32] Nasrollahzadeh, M., Sajadi, S. M., Rostami-Vartooni, A., Hussin, S. M. (2016). Green synthesis of CuO nanoparticles using aqueous extract of Thymus vulgaris L. leaves and their catalytic performance for N-arylation of indoles and amines. *Journal of colloid and interface science*, *466*, 113-119.

[33] Sharma, A., Dutta, R. K., Roychowdhury, A., Das, D., Goyal, A., & Kapoor, A. (2017). Cobalt doped CuO nanoparticles as a highly efficient heterogeneous catalyst for reduction of 4-nitrophenol to 4-aminophenol. *Applied Catalysis A: General*, *543*, 257-265.